Action-FRET: Probing the Molecular Conformation of Mass-Selected Gas-Phase Peptides with Förster Resonance Energy Transfer Detected by Acceptor-Specific Fragmentation

Steven Daly,*[†,‡] Frédéric Poussigue,[†,§] Anne-Laure Simon,[†,‡] Luke MacAleese,[†,‡] Franck Bertorelle,[†,‡] Fabien Chirot,[†,§] Rodolphe Antoine,[†,‡] and Philippe Dugourd[†,‡]

[†]Université de Lyon, F-69622 Lyon, France
[‡]Institut Lumière Matière, UMR5306, CNRS, Université Lyon 1, 69622 Villeurbanne, France
[§]Institut des Sciences Analytiques, UMR5280, CNRS, Université Lyon 1, 69100 Villeurbanne, France

Ⓢ Supporting Information

ABSTRACT: The use of Förster resonance energy transfer (FRET) as a probe of the structure of biological molecules through fluorescence measurements in solution is well-attested. The transposition of this technique to the gas phase is appealing since it opens the perspective of combining the structural accuracy of FRET with the specificity and selectivity of mass spectrometry (MS). Here, we report FRET results on gas-phase polyalanine ions obtained by measuring FRET efficiency through specific photofragmentation rather than fluorescence. The structural sensitivity of the method was tested using commercially available chromophores (QSY 7 and carboxyrhodamine 575) grafted on a series of small, alanine-based peptides of differing sizes. The photofragmentation of these systems was investigated through action spectroscopy, and their conformations were probed using ion mobility spectrometry (IMS) and Monte Carlo minimization (MCM) simulations. We show that specific excitation of the donor chromophore results in the observation of fragments that are specific to the electronic excitation of the acceptor chromophore. This shows that energy transfer took place between the two chromophores and hence that the action-FRET technique can be used as a new and sensitive probe of the structure of gas-phase biomolecules, which opens perspectives as a new tool in structural biology.
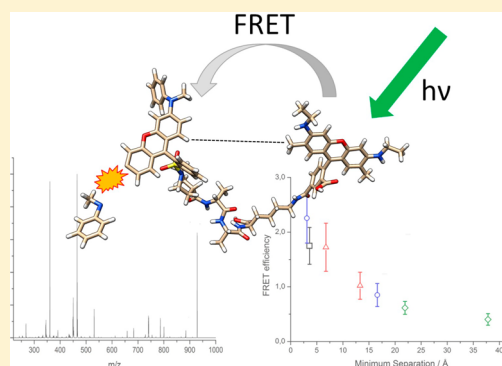
Förster resonance energy transfer (FRET) is a widely used probe of molecular structure in solution.[1−4] It requires a photon source to electronically excite the so-called "donor chromophore" and a light-harvesting setup to detect either the "donor" or "acceptor" chromophore fluorescence. The occurrence of FRET is then usually evidenced through a decrease in the fluorescence of the donor chromophore (quenching), with the concurrent onset of the fluorescence of the acceptor chromophore or by changes in fluorescence decay times. The interpretation of FRET results relies on the known distance dependence of the effect and on the possibility to graft specific chromophores at relatively well-defined sites on a molecule. FRET is then used to characterize the distance between the chromophores and hence separation between the grafting sites, although extracting exact distances is difficult due to the uncertainty of the exact orientation of the transition dipole moments of the chromophores. This allows the use of FRET to probe intra- or intermolecular distances, especially the change in distance, depending on whether the chromophores are attached to the same or to different molecules.

The versatility of FRET makes it a powerful tool to assess the conformation and/or association of molecules. It has been shown that the overall structure of complex molecular edifices can be preserved in the gas phase using soft ionization techniques.[5,6] Therefore, the development of techniques capable of probing FRET in the gas phase is of high interest and could be integrated into a global approach for structure determination of proteins and protein complexes.[7−9]

There are few techniques that allow structural investigation of large systems in vacuo.[10−12] One of the only techniques that can be successfully applied to large molecular edifices is ion mobility spectrometry (IMS), which provides global information on the overall shape of the system.[13−15] Associated with fluorescence spectroscopy, a few examples of gas-phase FRET have been recorded that very nicely demonstrate the possibility to observe and use FRET in the gas phase.[16−23]

However, fluorescence detectors are difficult to implement efficiently in mass spectrometers and their use has been limited to a small number of systems. Such "out-coupling" of light is difficult due to restriction of the solid angle of light detection imposed by the geometry of the mass spectrometer. By contrast, "in-coupling" of light—that is the coupling of a mass

spectrometer with a light source such as a laser—is simpler and has already been implemented by many groups.[24−27] The relative ease of "in-coupling" lends itself to an alternative methodology for monitoring the absorption of photons by ions in a mass spectrometer, namely, action spectroscopy. Action spectroscopy monitors the ion photodissociation as a function of the photon energy, and this photodissociation is assumed to be correlated to the absorption cross section of the ion. Action spectroscopy has been widely used to record the photo-dissociation spectra for a broad range of molecular ions and complexes across a large range of photon energies.[28−36] Due to the fact that detection of fragment ions is more sensitive than single-photon counting methods, such an action spectroscopy methodology for the measurement of FRET will provide a more sensitive probe of molecular structure of gas-phase biomolecules, simultaneously with usual mass spectrometry (MS) (including multistage) measurements.

In the following, we show that the high sensitivity of action spectroscopy can be used as a straightforward tool to detect FRET in the gas phase. A detection scheme will be presented that enables the measurement of FRET by fragment ion detection only.[37] Chromophores possessing a large overlap of the fluorescence spectrum of the "donor" with the absorption spectrum of the "acceptor", and with fragmentation of the "acceptor" specific to photodissociation, were chosen and characterized. Results on a series of alanine-based peptides of increasing size demonstrate the feasibility and sensitivity of the action-FRET methodology as a tool for the study of the structure of biomolecules in the gas phase.

■ EXPERIMENTAL AND THEORETICAL SECTION

Peptides and Chromophores. The choice of the peptides and chromophores will be discussed in greater detail in the following section. The acceptor chromophore is QSY7 *N*-succinimidyl ester (Life technologies), a dark quencher absorbing at 560 nm in solution and known to fragment efficiently at 532 nm in the gas phase.[38] The donor chromophore is 5-carboxyrhodamine 575 *N*-succinimidyl ester (rh575) (Life Technologies), absorbing at 550 nm and fluorescing at 575 nm in solution. Rh575 was also used as the donor chromophore by Talbot et al.[18], and both the fluorescence excitation and emission spectra along with photofragmentation mass spectra have been previously studied in detail.[39] Both chromophores are designed to be function-alized onto primary amines, and thus peptides containing two primary amine groups only were chosen. For the initial study, the simple tripeptide *N*-alanine−alanine−lysine−OH (AAK) was chosen to ensure that the chromophores remain spatially close to each other in the doubly grafted species. To study the distance dependence of the measured energy transfer, a series of polyalanine-based peptides varying in size from 7 to 19 residues were chosen with a lysine residue at both C- and N-terminus, the N-terminus being capped with an acetyl moiety to meet the condition of only two primary amines per molecule. Additionally, to aid the aqueous solubility histidine (H) was inserted at regular intervals along the chain. Thus, the following three peptides were chosen: KA_2HA_2K, KA_5HA_5K, and $KA_5HA_5HA_5K$.

The chromophores were grafted both individually and simultaneously onto the peptides. The two chromophores were dissolved in DMSO and the peptides in water, where the concentrations were approximately 10 mM in each case. *N*-Succinimidyl esters are reactive with water, and the hydrolysis is

competitive with the amide reaction required for grafting. Thus, it was necessary to use 500 μL of DMSO as the reactive medium for the grafting reactions. For the grafting of either donor or acceptor chromophore to the peptide (resulting in both singly and doubly grafted species) 10 μL of the chromophore and peptide solutions were added to the reaction medium. For the double grafting reaction with both chromophores, the volumes were adjusted to 14, 4, and 12 μL for rh575, QSY7, and peptide solutions, respectively, in order to optimize the grafting ratios. The reaction solutions were placed in an oven at 60 °C and left for at least 12 h, after which the solutions were tested to ensure the reaction was complete. It is important to note that it is possible for each chromophore to graft to the N-terminus or C-terminus primary amine, and thus there will be two doubly grafted species present: (rh575−peptide−QSY7) and (QSY7−peptide−rh575). Examination of the collision-induced dissociation (CID) mass spectra shows that both species are present in approximately equal amounts (see Supporting Information Figure S5). Separation of the two species is not possible; hence, all results on the doubly grafted species presented in this work are for this mixture of these two forms. For simplicity we will refer in the text to the doubly grafted species as (rh575−peptide−QSY7). For use in the electrospray ionization source, 20 μL of the reaction solution was diluted in 3 mL of 1:1 water/methanol with 3 μL acetic acid.

Mass Spectrometry and Optical Spectroscopy. The experimental setup used to perform the experiments presented in this paper has been described in detail previously.[40] Briefly, a linear quadrupole ion trap mass spectrometer (LTQ, Thermo Fisher Scientific, San Jose, CA) was used for ion preparation, ion selection and trapping, fragmentation (CID and photo-dissociation), and subsequent mass analysis. The back panel of the vacuum manifold was modified by drilling a hole and fitting a quartz window (30 mm diameter and 5 mm thickness). This window was positioned in front of the linear ion trap such as to allow the direct irradiation of trapped ions via a central hole in the trap exit electrode.

The light source used is a Panther EX OPO pumped by the third harmonic (355 nm) of a Surelite II Nd:YAG laser (Continuum, Santa Clara, CA). A repetition rate of 10 Hz and pulse widths of the order of 5 ns were used. The visible portion of the spectrum was used directly via the signal beam of the OPO (410−700 nm), which is collimated and refocused with a long focal distance lens of 500 mm. Pulse energies were kept between 0.9 and 1.1 mJ/pulse to avoid saturation. A mechanical shutter, synchronized with the mass spectrometer, is used to stop the beam at all times except the "ion activation window"—that is the time after ion accumulation and before the mass analysis. A single laser pulse was used for the irradiation of the trapped ions. When irradiating ions the normalized collision energy is kept at zero. Laser power is monitored continuously using the reflection portion of the beam upon passing through an 85:15 beam splitter placed at 45° with respect to the beam. The power is monitored using a power meter (Ophir-Spiricon GmbH, Ahrensburg, Germany). The value of the power used for normalization is taken as the average value over the duration of a measurement, of the order of 5 min per wavelength.

Ion Mobility Mass Spectrometry. Ion mobility measure-ments were performed using a custom-built ion mobility spectrometer already described elsewhere.[41] Briefly, a 1 m long drift tube is inserted between an electrospray ionization source and a time-of-flight (TOF) mass spectrometer. Helium at a

pressure of 15 Torr is maintained in the drift tube, and the temperature of the whole setup is kept at 300 K. Ions are periodically injected in the drift tube from an hourglass funnel ion trap. Their mass-to-charge ratio and drift time through the tube are simultaneously measured using the TOF. Ion mobilities and collision cross section (CCS) are finally calculated from the evolution of the ion arrival time distribution as a function of the inverse drift voltage.

Monte Carlo Simulations. Structures for the doubly grafted peptides were generated using a Monte Carlo minimization (MCM) approach using the Tinker[42] suite of programs. The choice of force field is constrained by the requirement that the entire system be modeled, and as such the MMFF94 force field[43] was chosen as the most suitable to account for all the necessary parameters. Initial geometries were chosen with all peptide dihedral angles in the trans configuration. For the higher charge states, protons were placed on both the histidine and carboxy moieties. For the lower charge state, one of the additional protons was removed from either the C- terminus or Rh575 carboxy moiety, or from histidine.

Additionally, the two possible doubly grafted species discussed above (donor or acceptor grafted at the N-terminus) were considered. Two observables were extracted from these calculated structures in order to compare to the experimental measurements. The CCSs for simulated structures were calculated in the Mobcal suite of programs using the trajectory method with standard parameters.[44] The interchromophore distance was also extracted calculated as the minimum distance between any two atoms (excluding hydrogen) in the optically active portion of the chromophores (defined as the xanthene moiety plus the side chains).

■ RESULTS AND DISCUSSION

Various processes are involved in action-FRET: the resonant energy transfer itself, as well as the competing radiative and nonradiative relaxation mechanism of both acceptor and donor chromophore. Thus, FRET relies on the choice of a suitable chromophore pair. In order to observe FRET in solution, the chromophores must have clearly resolved absorption bands and there must be a significant overlap of the donor fluorescence spectrum and acceptor absorption spectrum.

Moreover, the resonant energy transfer must happen on a shorter time scale than the relaxation of the donor chromophore. Similar constraints exist for action-FRET in the gas phase, with the additional constraints that the acceptor chromophore must have a fragmentation pattern that is specific to electronic excitation and that is different from statistical fragmentation that occurs after heating (for example, by CID or IRMPD). Therefore, acceptor fragmentation must happen on a shorter time scale than fluorescence and the statistical redistribution of the energy over the entire molecule. Thus, in the doubly grafted species, by monitoring the laser-induced dissociation (LID), we conclude that the observation of two absorption bands is due to FRET. It is also important to show that the strength of the observed action-FRET depends on the distance between the two chromophores.

Figure 1 shows the action spectra for mass-selected (rh575)+ (black squares) and (QSY7)+ (red circles), measured as total fragmentation yield. There is an obvious difference in the amplitude of the fragmentation yield of the two chromophores. Since rh575 has a high quantum yield (0.83 in ethanol) the primary relaxation mechanism can be expected to be
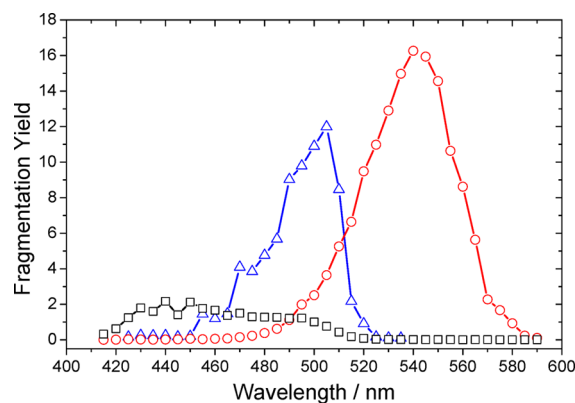

Figure 1. Action spectra of mass-selected (QSY7)+ (red circles), (rh575)+ (black squares), and (rh575−AAK−rh575)2+ (blue triangles). Fragmentation yields are calculated from data measured in comparable experimental conditions and normalized with respect to the laser power.

fluorescence at the maximum of absorption, which has been shown to be $\lambda = 495$ nm in the gas phase.[39,45] Hence, the action spectrum in this case is weak due to fragmentation being a relatively minor relaxation mechanism, and thus the expected absorption maximum is not observed. As QSY7 is a dark quencher, fluorescence is not available as a relaxation mechanism, and hence, it fragments efficiently. In both cases, the fragmentation yield was measured as a function of power and showed a quadratic dependence indicating that the fragmentation is a two-photon process. This is consistent with previous study of the photofragmentation of rhodamines, which shows the same quadratic dependence at low power.[39] For measurement of all spectra presented here, the average power at each wavelength is kept between 0.9 and 1.1 mW.

The blue triangles in Figure 1 show the action spectrum of mass-selected (rh575−AAK−rh575)2+. It is a well-known property of rhodamines that there is a large reduction in the fluorescence quantum yield upon the formation of clusters of rhodamine molecules.[46] Hence, there is a decrease in the importance of fluorescence as a relaxation mechanism, and a concurrent increase in the fragmentation yield is observed for (rh575−AAK−rh575)2+. This confirms the interpretation that the nonobservance of the expected absorption maximum in the fragmentation yield of (rh575)+ is explained by the competition of fluorescence and fragmentation. It also suggests that the action spectrum of (rh575−AAK−rh575)2+ can be used as a proxy for the absorption spectrum of (rh575)+. Indeed, the position of the peak of $\lambda = 505$ nm for (rh575−AAK−rh575)2+ compares favorably with the value of $\lambda = 495$ nm found in previous in vacuo measurements.[18,39] As a conclusion of the action spectroscopy studies, rh575 and QSY7 satisfy the first condition required for FRET: that the absorption bands are clearly distinguished, with absorption maxima of $\lambda_D = 505$ nm and $\lambda_A = 545$ nm, respectively.

Additionally, donor (rh575) emission as observed in the gas phase[39] and acceptor (QSY7) absorption spectra show a large overlap. Thus, these two chromophores are well-suited for FRET in the gas phase.

It must still be established that the fragmentation observed for the acceptor chromophore is LID-specific so that one can discriminate the origin of the excitation. Figure 2 shows the mass spectra of mass-selected (AAK−QSY7)+ following CID (top) and LID at $\lambda_A = 545$ nm (bottom), respectively. There is
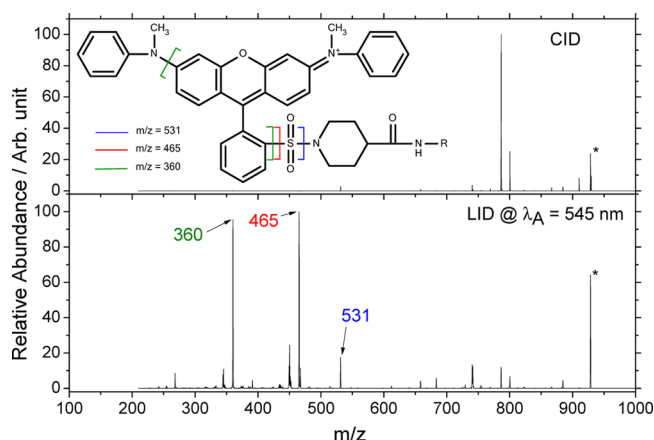
Figure 2. Mass spectra of mass-selected (QSY7-AAK)$^+$ ions following CID (top panel) and LID at λ_A = 545 nm (bottom panel). The asterisk denotes the precursor ion. The top panel shows the structure of the (QSY7)$^+$ ion, the R group representing the grafting location onto the peptide. The solid lines indicate the bonds broken to give rise to the major fragments observed in the LID mass spectrum.

clearly a large difference in the fragmentation pattern observed due to either heating or electronic excitation. The fragments observed in CID correspond to fragmentation of the peptide backbone. Conversely, the LID mass spectrum is dominated by two fragments at m/z 465 and 360, which correspond to the breaking of the S−C bond alone and combined breaking of the C−N bond between the xanthene and N-methylaniline moiety, see the inset of Figure 2. These two latter fragments are not observed in CID, and their observation is thus a clear signature that QSY7 has been electronically excited. It is therefore possible to follow FRET by measuring the relative intensity of these fragments as a function of wavelength for the doubly grafted peptides.

Figure 3 shows the result of this procedure for mass-selected (rh575−AAK−QSY7)$^{2+}$, giving an action spectrum where only
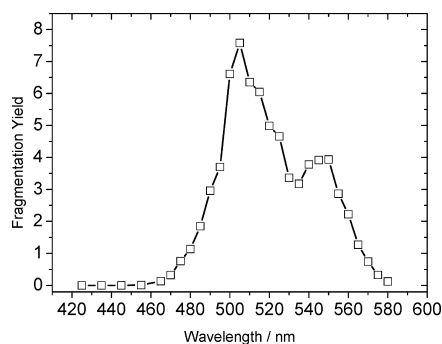

Figure 3. Action spectrum of mass-selected (rh575−AAK−QSY7)$^{2+}$. The fragmentation yield here has been determined using only the LID-specific fragments as shown in Figure 2.

the LID-specific acceptor fragments noted above are monitored. If there were no energy transfer, the same action spectrum as the one shown in Figure 1 for QSY7 would be expected. However, there are clearly two bands present in the spectrum: one at 545 nm corresponding to absorption of the acceptor chromophore, and one at 505 nm which is in the region where the donor chromophore was found to absorb. Observation of the donor chromophore absorption band via measurement of fragments specific to electronic excitation of

the acceptor chromophore is direct evidence for electronic energy transfer having occurred.

Considering the data presented in Figures 1−3, it is possible to make some general comments about the relative time scales of the processes occurring following photoexcitation. First, the action spectrum of (rh575)$^+$ ions indicates that fluorescence from the excited state occurs on a shorter time scale than either photofragmentation or internal vibrational redistribution (IVR), which is in full agreement with the high fluorescence quantum yield and a fluorescence lifetime of 5.65 ± 0.04 ns in vacuo.[47] Second, the high fragmentation yields observed in (AAK−QSY7)$^+$ and the large difference in the observed fragmentation following CID and LID indicates that photofragmentation of (QSY7)$^+$ occurs on a shorter time scale than IVR. Finally, the observation of FRET in (rh575−AAK−QSY7)$^{2+}$ indicates that FRET must occur on a shorter time scale than fluorescence of (rh575)$^+$, and again that the subsequent photofragmentation of (QSY7)$^+$ must occur on a shorter time scale than IVR. These results are completely consistent with previous fluorescence lifetime measurements of donor−peptide−acceptor systems.[18] An additional important point to note is that the rate of IVR will increase as the length of the peptide is increased. As system size increases there, competition between IVR and direct photofragmentation of the acceptor chromophore may arise. As a consequence of this competition, the overall LID-specific fragmentation intensity can be expected to decrease relative to the intensity of the statistical fragments. This competition between IVR and photofragmentation will exist as soon as the energy is localized on the acceptor chromophore regardless of the origin of this energy: photofragmentation following FRET or following direct absorption will be equally affected. Therefore, if the FRET-mediated photofragmentation of the acceptor chromophore is normalized by the direct photofragmentation, an IVR-independent quantification of action-FRET can be effected.

This discussion lends itself to the following definition of the action-FRET efficiency. The absorption due to the acceptor chromophore is independent of the system in terms of peak position and shape, with a spectrum resembling that shown in Figure 1 being recorded when the acceptor chromophore is individually grafted onto each of the peptides used.

Thus, it is possible to take the ratio of the area of the peaks due to the donor and acceptor absorptions as a relative measure of the FRET efficiency. When this procedure is performed on the data for (rh575−AAK−QSY7)$^{2+}$ (see Supporting Information Figure S8) a value of 1.75 ± 0.34 is obtained, where the error is determined from the error in the fit. Measurements of the action spectra and an identical fitting procedure were performed on doubly grafted KA$_2$HA$_2$K, KA$_5$HA$_5$K, and KA$_5$HA$_5$HA$_5$K (see Supporting Information Figures S9−S14). Two charge states were observed in each case: 2+ and 3+ for (rh575−KA$_2$HA$_2$K−QSY7) and (rh575−KA$_5$HA$_5$K−QSY7) and 3+ and 4+ for (rh575−KA$_5$HA$_5$HA$_5$K−QSY7). Values of the FRET efficiency between 0.40 and 2.25 were measured for these species.

To investigate the relationship between the FRET efficiency and the chromophore separation—and hence the structure of the peptides—an independent determination of the structure of the doubly grafted peptides was obtained by measurement of the CCS using IMS and use of MCM simulations for each charge state of the doubly grafted peptides, see Table 1 and Figure 4. It was not possible to measure experimentally the CCS values for the largest peptide, KA$_5$HA$_5$HA$_5$K, due to a low

Table 1. Experimental and Calculated Collision Cross Sections and FRET Efficiency of Doubly Grafted Peptides

peptide	charge	MCM CCS Å²	exptl CCS Å²	FRET efficiency
AAK	2+	337 ± 4	324	1.75 ± 0.12
KA_2HA_2K	3+	445 ± 3	508	1.02 ± 0.25
	2+	374 ± 3	377	1.72 ± 0.44
KA_5HA_5K	3+	518 ± 7	557	0.85 ± 0.21
	2+	452 ± 4	467	2.25 ± 0.45
$KA_5HA_5\ HA_5K$	4+	624 ± 5		0.40 ± 0.10
	3+	635 ± 4		0.61 ± 0.11

total ion signal. Examination of the IMS profiles suggests a single conformational family is present for each of the systems studied, which is consistent with the observation of a single low-energy conformational family in the MCM data. These conformational families possess the same peptide backbone structure, but differ in the orientation of the chromophores. To account for these conformational families, average values for the cross section and minimum chromophore separation— weighted by the relative energy of each conformer—were used. It is also important to note that the calculations for both doubly grafted species (rh575−peptide−QSY7) and (QSY7− peptide−rh575) were performed, and in each case the peptide backbone structure of the lowest energy conformational family was identical. Examination of Table 1 shows that there is in general a good agreement between the calculated and experimental CCS values for each species. It should be noted that there is an underestimation of the CCS for the 3+ charge

state of the peptides, suggesting that the calculated structures are too compact which will lead to an underestimation of the minimum chromophore separation. Nonetheless, it is clear that each doubly grafted peptide becomes more extended as the charge state is increased from 2+ to 3+. This is consistent with the intuitive expectation that Coulomb repulsion would cause unfolding at higher charge states, causing a concurrent increase in the chromophore separation. Indeed, in the 2+ charge state of the doubly grafted peptides, it is the two chromophores that carry the positive charges. In the 3+ charge state, the proton is added to the histidine side chain and the additional Coulomb repulsion forces the chromophores apart (see Figure 4a−d). In the case of doubly grafted $KA_5HA_5HA_5K$ the 3+ and 4+ charge states are observed, corresponding to protonation of one and two histidine side chains, respectively (Figure 4, parts e and f). Both charge states are calculated to have an extended structure with the main difference being the uncoiling of the helical motif of the five alanine residues situated between the two histidine residues. It can be concluded from the comparison of experimental and calculated CCS that the calculated structures are representative of the doubly grafted peptides, and thus we can examine the dependence of the FRET efficiency on the minimum chromophore separation, as defined above.

Figure 5 shows the FRET efficiency against minimum chromophore separation for all doubly grafted species examined (see Table 1 for the numerical values). It is clear that there is a monotonic decrease in the FRET efficiency as the separation of the chromophores is increased. The FRET efficiency of the higher charge state is consistently less than that
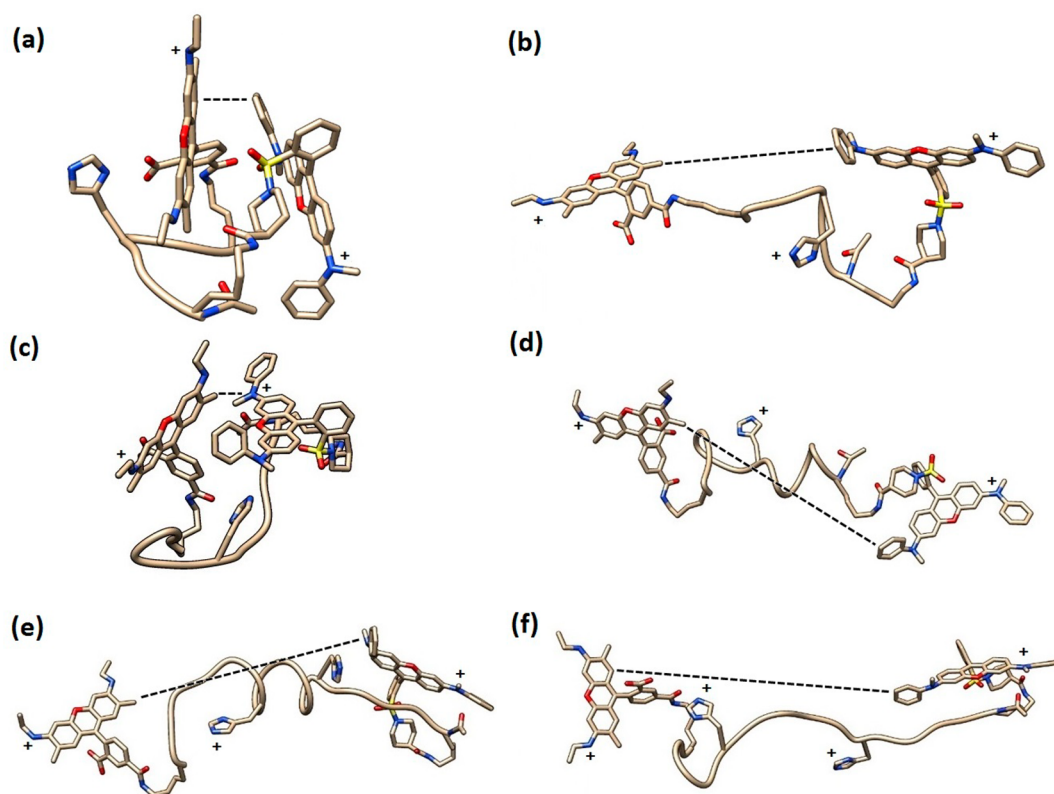

Figure 4. Lowest energy MCM structures for (a) (rh575−KA₂HA₂K−QSY7)²⁺, (b) (rh575−KA₂HA₂K−QSY7)³⁺, (c) (rh575−KA₅HA₅K−QSY7)²⁺, (d) (rh575−KA₅HA₅K−QSY7)³⁺, (e) (rh575−KA₅HA₅HA₅K−QSY7)³⁺, and (f) (rh575−KA₅HA₅HA₅K−QSY7)⁴⁺. The positions of the positive charges for each species are indicated on the figure. The dashed line shows the minimum separation of the chromophores and corresponds to the minimum distance between any two heavy atoms on the optically active region of the chromophore.
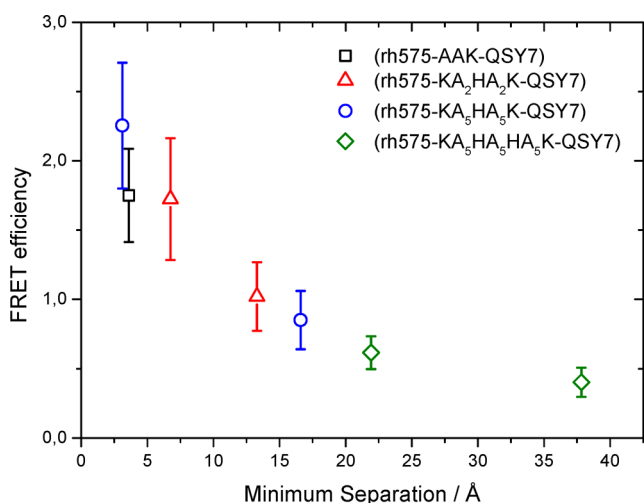
Figure 5. FRET efficiency vs average value of the minimum chromophore separation for the different charge states of doubly grafted AAK (squares), KA_2HA_2K (triangles), KA_5HA_5K (circles), and $KA_5HA_5HA_5K$ (diamonds).

of the lower charge state, for each peptide size, which is consistent with the CCS data presented above.

In particular the large change in structure—from globular to extended—that is observed with the addition of a proton for doubly grafted KA_2HA_2K and KA_5HA_5K leads to an equally large change in the FRET efficiency: from 1.72 ± 0.44 to 1.02 ± 0.25 in KA_2HA_2K and from 2.25 ± 0.45 to 0.85 ± 0.21 in KA_5HA_5K.

The situation for doubly grafted $KA_5HA_5HA_5K$ is interesting as the MCM calculations suggest that there is not a large change in the global shape as the charge state is increased from 3+ to 4+. This is reflected in the small change in the calculated values of the CCS from 624 to 635 Å^2. However, there is a proportionally greater change in the value of the FRET efficiency: 0.61 ± 0.11 for the 3+ and 0.40 ± 0.10 for the 4+ charge state, respectively. This suggests that the action-FRET is more sensitive to such local changes in structure—in this case the uncoiling of the central five alanine residues—than is IMS, and therefore the two techniques are able to provide complementary information. Overall, these data are in agreement with previous results on the structure of gas-phase multicharged polyalanines, showing that chromophores have limited influence on the structure of the peptides.[48,49]

A final point to note is that it is possible to measure the action FRET by performing measurement of the LID spectrum at only two wavelengths: λ_D and λ_A. In such a case, the FRET efficiency would be defined as the ratio of the fragmentation yield of acceptor fragments measured at λ_D and λ_A. If this procedure is performed on the data presented in this paper, identical trends are observed.

CONCLUSION

We have proposed a scheme for the measurement of FRET in the gas phase using a method based only on fragment ion detection. The principal features that would have to be identified for such an action-FRET scheme were discussed and subsequently shown experimentally. A dark-quenching chromophore, QSY7, was identified and its fragmentation characterized to show that there were fragments specific to electronic excitation. A suitable fluorescent donor chromo-

phore, rh575, was identified and characterized. Measurement of the action spectrum of the two chromophores both grafted onto the simple tripeptide AAK showed that the absorption maximum of rh575 is observed via measurement of the fragments specific to the electronic excitation of QSY7. Thus, it was possible to conclude that the energy had been transferred from the donor to acceptor chromophore. It was also possible to conclude that the FRET observed must occur on a shorter time scale than both the fluorescence of the donor and the internal vibrational redistribution of energy across the entire molecule. It was also possible to define an IVR-independent quantification of the FRET efficiency considering the photofragmentation efficiency following FRET and direct absorption of the acceptor chromophore.

This definition of the FRET efficiency—taken as the ratio of the area of the peaks in the action spectrum due to absorption of the donor and acceptor chromophores—was used in conjunction with measurements of the collision cross section via IMS and MCM simulations on a series of polyalanine-based peptides containing between 7 and 19 amino acids. It was shown that there is a clear dependence on the magnitude of the FRET efficiency observed with the separation of the chromophores in each the system studied. Comparison with MCM simulations showed that the FRET efficiency is well-correlated with an increase in the separation of donor and acceptor chromophores. Hence, the action-FRET methodology set out in the paper is suitable for gas-phase studies of the structure of biomolecules and provides orthogonal information to IMS measurements as it is sensitive to a distance between two defined parts of the molecular ion, while IMS is sensitive to the global shape. The action-FRET methodology provides a significant advance in the study of the conformation and structure of gas-phase molecular ions. This method therefore has a strong potential in native MS as part of a global approach in structural biology.

ASSOCIATED CONTENT

Ⓢ Supporting Information
CID and LID mass spectra of singly and doubly grafted AAK, identification of the internal chromophore fragments, fitted raw action spectra for all doubly grafted species, MCM structures of doubly grafted three-residue peptide. This material is available free of charge via the Internet at http://pubs.acs.org.

AUTHOR INFORMATION

Corresponding Author
*E-mail: steven.daly@univ-lyon1.fr.
Notes
The authors declare no competing financial interest.

ACKNOWLEDGMENTS

REFERENCES

(1) Weiss, S. *Science* **1999**, *283*, 1676.
(2) Selvin, P. R. *Nat. Struct. Biol.* **2000**, *7*, 730.
(3) Schuler, B.; Lipman, E. A.; Eaton, W. A. *Nature* **2002**, *419*, 743.
(4) Giepmans, B. N. G.; Adams, S. R.; Ellisman, M. H.; Tsien, R. Y. *Science* **2006**, *312*, 217.

(5) Ruotolo, B. T.; Robinson, C. V. *Curr. Opin. Chem. Biol.* **2006**, *10*, 402.

(6) van den Heuvel, R. H.; Heck, A. J. R. *Curr. Opin. Chem. Biol.* **2004**, *8*, 519.

(7) Miranker, A.; Robinson, C. V.; Radford, S. E.; Aplin, R. T.; Dobson, C. M. *Science* **1993**, *262*, 896.

(8) Heck, A. J. R. *Nat. Methods* **2008**, *5*, 927.

(9) Vonhelden, G.; Wyttenbach, T.; Bowers, M. T. *Science* **1995**, *267*, 1483.

(10) Sinz, A. *Mass Spectrom. Rev.* **2006**, *25*, 663.

(11) Konermann, L.; Pan, J. X.; Liu, Y. H. *Chem. Soc. Rev.* **2011**, *40*, 1224.

(12) Breuker, K.; Oh, H. B.; Horn, D. M.; Cerda, B. A.; McLafferty, F. W. *J. Am. Chem. Soc.* **2002**, *124*, 6407.

(13) Bleiholder, C.; Dupuis, N. F.; Wyttenbach, T.; Bowers, M. T. *Nat. Chem.* **2011**, *3*, 172.

(14) Bush, M. F.; Hall, Z.; Giles, K.; Hoyes, J.; Robinson, C. V.; Ruotolo, B. T. *Anal. Chem.* **2010**, *82*, 9557.

(15) Uetrecht, C.; Rose, R. J.; van Duijn, E.; Lorenzen, K.; Heck, A. J. R. *Chem. Soc. Rev.* **2010**, *39*, 1633.

(16) Danell, A. S.; Parks, J. H. *Int. J. Mass Spectrom.* **2003**, *229*, 35.

(17) Dashtiev, M.; Azov, V.; Frankevich, V.; Scharfenberg, L.; Zenobi, R. *J. Am. Soc. Mass Spectrom.* **2005**, *16*, 1481.

(18) Talbot, F. O.; Rullo, A.; Yao, H.; Jockusch, R. A. *J. Am. Chem. Soc.* **2010**, *132*, 16156.

(19) Frankevich, V.; Guan, X. W.; Dashtiev, M.; Zenobi, R. *Eur. J. Mass Spectrom.* **2005**, *11*, 475.

(20) Iavarone, A. T.; Meinen, J.; Schulze, S.; Parks, J. H. *Int. J. Mass Spectrom.* **2006**, *253*, 172.

(21) Iavarone, A. T.; Patriksson, A.; van der Spoel, D.; Parks, J. H. *J. Am. Chem. Soc.* **2007**, *129*, 6726.

(22) Shi, X. G.; Duft, D.; Parks, J. H. *J. Phys. Chem. B* **2008**, *112*, 12801.

(23) Frankevich, V.; Chagovets, V.; Widjaja, F.; Barylyuk, K.; Yang, Z. Y.; Zenobi, R. *Phys. Chem. Chem. Phys.* **2014**, *16*, 8911.

(24) Bowers, W. D.; Delbert, S. S.; Hunter, R. L.; McIver, R. T. *J. Am. Chem. Soc.* **1984**, *106*, 7288.

(25) Vanderhart, W. J. *Mass Spectrom. Rev.* **1989**, *8*, 237.

(26) Dunbar, R. C. *Int. J. Mass Spectrom.* **2000**, *200*, 571.

(27) Brodbelt, J. S. *Chem. Soc. Rev.* **2014**, *43*, 2757.

(28) MacAleese, L.; Maitre, P. *Mass Spectrom. Rev.* **2007**, *26*, 583.

(29) Drayss, M. K.; Blunk, D.; Oomens, J.; Polfer, N.; Schmuck, C.; Gao, B.; Wyttenbach, T.; Bowers, M. T.; Schafer, M. *Int. J. Mass Spectrom.* **2009**, *281*, 97.

(30) Case, A. S.; Heid, C. G.; Western, C. M.; Crim, F. F. *J. Chem. Phys.* **2012**, *136*, 8.

(31) Crampton, K. T.; Rathur, A. I.; Nei, Y. W.; Berden, G.; Oomens, J.; Rodgers, M. T. *J. Am. Soc. Mass Spectrom.* **2012**, *23*, 1469.

(32) Wyer, J. A.; Jensen, C. S.; Nielsen, S. B. *Int. J. Mass Spectrom.* **2011**, *308*, 126.

(33) Yao, H.; Jockusch, R. A. *J. Phys. Chem. A* **2013**, *117*, 1351.

(34) Klaerke, B.; Holm, A. I. S.; Andersen, L. H. *Astron. Astrophys.* **2011**, *532*, 5.

(35) Hansen, C. S.; Kirk, B. B.; Blanksby, S. J.; O'Hair, R. A. J.; Trevitt, A. J. *J. Am. Soc. Mass Spectrom.* **2013**, *24*, 932.

(36) Kirk, B. B.; Trevitt, A. J.; Blanksby, S. J.; Tao, Y. Q.; Moore, B. N.; Julian, R. R. *J. Phys. Chem. A* **2013**, *117*, 1228.

(37) Macaleese, L.; Chirot, F.; Bazus, L.; Bertorelle, F.; Antione, R.; Lemoine, J.; Dugourd, P. Presented at the 60th ASMS Conference on Mass Spetrometry and Allied Topics, Vancouver, BC, Canada, May 20−24, 2012.

(38) Enjalbert, Q.; Girod, M.; Simon, R.; Jeudy, J.; Chirot, F.; Salvador, A.; Antoine, R.; Dugourd, P.; Lemoine, J. *J. Anal. Bioanal. Chem.* **2013**, *405*, 2321.

(39) Forbes, M. W.; Jockusch, R. A. *J. Am. Soc. Mass Spectrom.* **2011**, *22*, 93.

(40) Larraillet, V.; Antoine, R.; Dugourd, P.; Lemoine, J. *Anal. Chem.* **2009**, *81*, 8410.

(41) Albrieux, F.; Calvo, F.; Chirot, F.; Vorobyev, A.; Tsybin, Y. O.; Lepere, V.; Antoine, R.; Lemoine, J.; Dugourd, P. *J. Phys. Chem. A* **2010**, *114*, 6888.

(42) TINKER Molecular Modeling Web site. http://dasher.wustl.edu/tinker.

(43) Halgren, T. A. *J. Comput. Chem.* **1996**, *17*, 490.

(44) Mesleh, M. F.; Hunter, J. M.; Shvartsburg, A. A.; Schatz, G. C.; Jarrold, M. F. *J. Phys. Chem.* **1996**, *100*, 16082.

(45) Arbeloa, F. L.; Arbeloa, T. L.; Lage, E. G.; Arbeloa, I. L.; Deschryver, F. C. *J. Photochem. Photobiol., A* **1991**, *56*, 313.

(46) McRae, E. G.; Kasha, M. *J. Chem. Phys.* **1958**, *28*, 721.

(47) Nagy, A. M.; Talbot, F. O.; Czar, M. F.; Jockusch, R. A. *J. Photochem. Photobiol., A* **2012**, *244*, 47.

(48) Hudgins, R. R.; Jarrold, M. F. *J. Am. Chem. Soc.* **1999**, *121*, 3494.

(49) Counterman, A. E.; Clemmer, D. E. *J. Phys. Chem. B* **2003**, *107*, 2111.